TECHNICAL PAPER

Numerical and experimental investigations of mixing length in square wave serpentine micromixer with obstacles

Bappa Mondal[1,2] · Promod Kumar Patowari[2] · Sukumar Pati[2]

Abstract

In the present work, numerical and experimental investigations have been carried out to characterize the fluid mixing and pressure drop through square wave serpentine passive micromixers with obstacles at different inlet flow conditions. Three different shapes of obstacles, viz., rectangular, triangular and semicircular are introduced along the walls of the micromixer. Based on the simulation results, the most effective design micromixer is proposed. The results show that introducing obstacles in the micromixer enhances the mixing performance at the cost of higher pressure drop. It further reveals that the mixing performance is the highest for micromixer with triangular obstacles and the pressure drop is also the lowest among all the micromixers with obstacles. Finally, the computational results are validated with the experimental results.

1 Introduction

The research investigations in the area of micro-scale mixing have received huge momentum in last few decades because of wide applications in clinical diagnostics such as protein folding, drug delivery, biochemical reactions, cells shorting, DNA sequencing, chemical analysis, enzyme reactions etc. (Nguyen and Wu 2005; Rashidi et al. 2018; Lee and Fu 2018; Bayareh et al. 2020; Mehta et al. 2022; Mehta and Pati 2022). The development of microfluidic devices is essential to achieve prompt results with utmost accuracy in medical diagnostics. With the development of microfluidic devices, a clinical laboratory may be integrated into the form of a single-chip (Connolly 1995). One could achieve various advantages such as reduced cost, lesser sample volume, quick result, high precision, automatic measurement, improved analysis, laboratory safety, etc., by reducing the size of clinical systems (Jakeway et al. 2000).

Mixing of two or more fluids homogeneously in an efficient manner within a short period of time is essential in several applications although it is a challenging task (Miranda et al. 2010). The flow in most of the microfluidic devices is laminar in nature. Accordingly, the mixing is guided by molecular diffusion and chaotic advection. It can be noted that the diffusion time (t) is inversely proportional to the diffusion coefficient (D). As the diffusion coefficient is low for most of the fluids, long mixing length and extensive mixing time are required for achieving uniform mixing (Kunti et al. 2017). Several enhanced microfluidic devices have been developed to overcome the difficulties to date in this issue. Based on the mechanism of the mixing, micromixers are classified as active and passive ones. Researchers have found that active micromixer induces turbulent flows either by using moving parts or an external power source such as an electric field (Kunti et al. 2018; Mondal et al. 2021; Vasista et al. 2022), magnetic field (Ballard et al. 2016), acoustics (Ang et al. 2016), pressure, hydrodynamics (Deshmukh et al. 2000), ultrasonic effects (Yang et al. 2001), thermal

✉ Sukumar Pati
sukumar@mech.nits.ac.in

Bappa Mondal
bappamondalme@gmail.com

Promod Kumar Patowari
ppatowari@mech.nits.ac.in

1   Department of Mechanical Engineering, GMR Institute of Technology, Rajam, Andhra Pradesh 532127, India

2   Department of Mechanical Engineering, National Institute of Technology Silchar, Silchar, Assam 788010, India

or mechanical power (Huang and Tsou 2014), etc. In passive micromixers, no external energy source other than the pumping power is used to improve the mixing. To improve the mixing efficiency between Ferro-nanofluid and water in a Y-type semi-active micromixers, a permanent magnet is placed in an appropriate position near the microchannels (Tsai et al. 2009). The prime reasons for wide applications of passive micromixers are easy to fabricate and handle due to less complexity, and inexpensive.

Moreover, to achieve better mixing, passive micromixers have been modified by changing the geometry of the channel (Mondal et al. 2019a, 2020a, b). Ribbed surface and different shape of obstacles have been added in the channel geometry to improve the mixing performance (Borgohain et al. 2018a, b; Wangikar et al. 2018; Mondal et al. 2019b, 2020c). The mixing quality increases with increasing the confluence angle between the inlets and flow rate ratio (Mondal et al. 2018, 2020d). By increasing the asymmetry level of the inlets, mixing quality improves to a significant extent (Calado et al. 2016). Several researchers have proposed passive micromixers with lateral obstructions along the microchannel arranged both symmetric and asymmetric way. Several researchers (Khosravi Parsa et al. 2014; Gambhire et al. 2016; Chen et al. 2016; Sarma and Patowari 2017; Borgohain et al. 2018a; Mondal et al. 2019a) have studied the influence of micromixer geometry on the mixing efficiency and pressure drop using numerical and experimental investigations. Three different geometries: a square-wave mixer, a three-dimensional serpentine mixer and a staggered herringbone mixer are designed and analyzed for improving the mixing efficiency. Better mixing efficiency is obtained in serpentine micro-channel as compared to the straight microchannel (Das et al. 2017).

A group of researchers (Falk and Commenge 2010; Commenge and Falk 2011; Pinot et al. 2014; Pérez et al. 2020) have carried out extensive research works in the field of micromixing. They showed extensive comparison of mixing efficiency of various types of micromixers. Considering simple relations of mixing in laminar flow, it was observed that to obtain the theoretical mixing time and how to relate it with functioning parameters as the Reynolds number of the flow and the specific power dissipation per mass unit of fluid. They compared the experimental and theoretical mixing times and pointed out that only a few percents of the total mechanical power transmitted to the fluid is effective for mixing. Moreover, to characterize micromixing in conventional stirred tank reactor, they proposed iodide/iodate chemical test reaction named Villermaux–Dushman method.

Several numerical, as well as experimental studies, have been reported in literature analyzing the mixing performance of passive micromixers considering the effect of corrugated shape and obstacles along the channel. However, square wave micromixer with obstacles has not been considered to analyze the performance. In the present work, mixing performance and pressure drop are analyzed both numerically and experimentally in a square wave micromixer with obstacles of three different shape. The results have been parameterized in terms of mixing length, density difference and pressure drop. For experimentation purpose, channels have been fabricated with developed techniques and then experimentally analyzed the mixing of fluid at different flow conditions.

2 Problem specification

Figure 1 illustrates a serpentine square wave micromixer without any obstacle. It consists of two inlets which are placed at 90º to each other. The width and the depth of the micromixer are 300 μm and 300 μm, respectively. The side length of the micromixer is 1200 μm. Three different serpentine square wave micromixers with obstruction in channel width are also designed. The geometries of the obstacles are rectangular, triangular and semicircular. Serpentine square wave micromixer with rectangular, triangular and semicircular shaped obstructions are shown in Fig. 2. Water and ethyl alcohol are taken as the input fluid for mixing. A comparison study has been carried out on the mixing performance of the following four variants of micromixer:
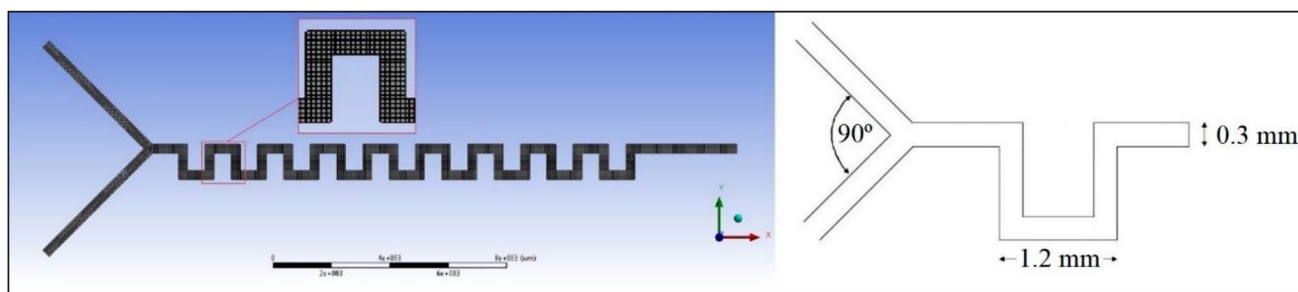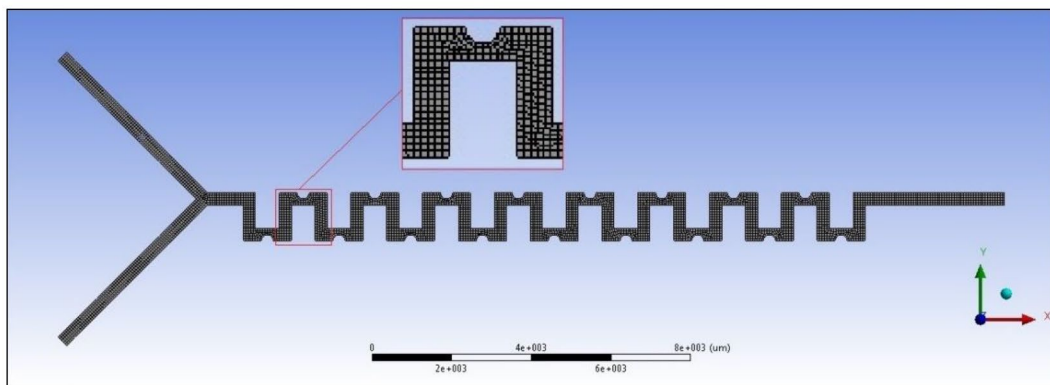

Fig. 1 Serpentine square wave micromixer
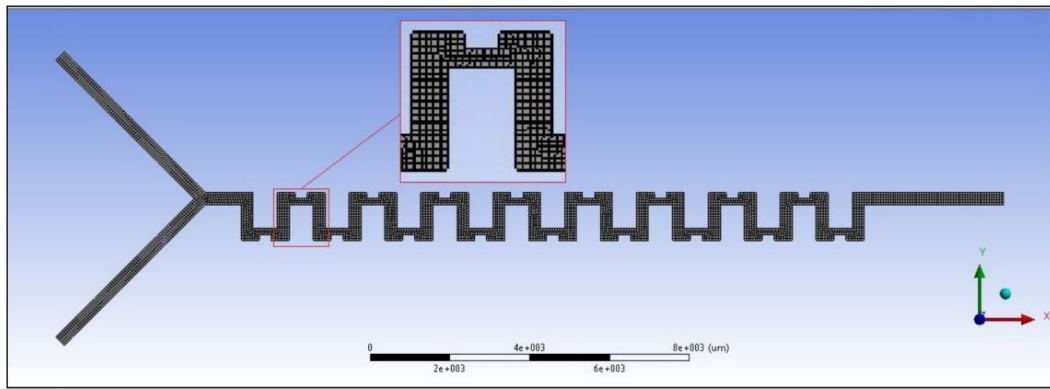
(a)
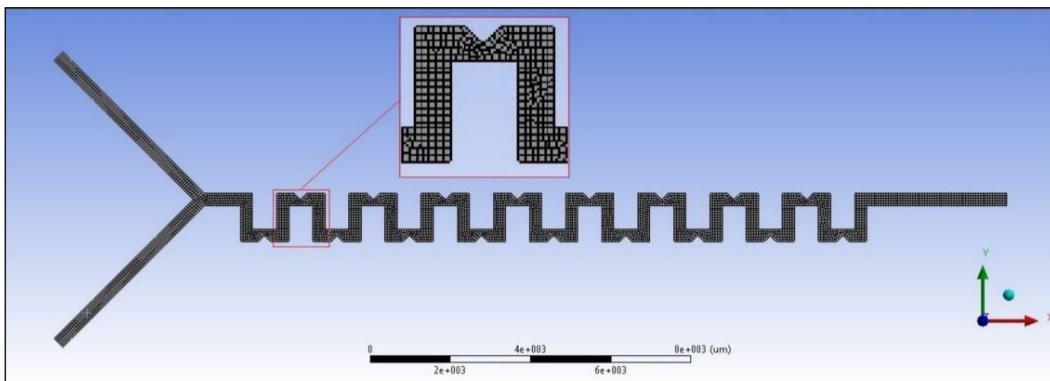
(b)

(c)

Fig. 2 Serpentine square wave micromixers with different shapes of obstacles (**a**) rectangular, (**b**) triangular and (**c**) semicircular

- A Serpentine square wave type micromixer (S0 type).
- A serpentine square wave with rectangular obstruction type micromixer (S1 type).
- A serpentine square wave with triangular obstruction type micromixer (S2 type).
- A serpentine square wave with semicircular obstruction type micromixer (S3 type).

3 Theoretical formulation

In this work, flow is laminar, incompressible and steady, and both the working fluids are Newtonian. The equations of mass, momentum, and species conservations are as follows:

Mass conservation

$$\vec{\nabla} \cdot \vec{V} = 0 \tag{1}$$

Momentum conservation

$$(\vec{V} \cdot \vec{\nabla})\vec{V} = -\frac{1}{\rho}\nabla p + \upsilon\nabla^2\vec{V} \tag{2}$$

Species conservation

$$(V \cdot \nabla)C = D\nabla^2 C \tag{3}$$

where ρ is the density of the fluid, V is the velocity of the fluid, v is kinematic viscosity, D the diffusion coefficient and C is the concentration.

The boundary simulations are as follows.

Table 1 Grid independence test for different geometry (at inlet velocity 0.003 m/s)

Geometry	Mesh	No of elements	Density difference at location 4	Error (%)
S0 type	M1	25074	4.25	3.41
	M2	47521	4.348	1.18
	M3	82547	4.398	0.05
	M4	109548	4.4	-
S1 type	M5	25388	0.5343	2.95
	M6	48104	0.51	1.73
	M7	81345	0.5149	0.79
	M8	111024	0.519	-
S2 type	M9	26045	0.2178	2.25
	M10	47892	0.2164	1.60
	M11	83583	0.2124	0.28
	M12	110389	0.213	-
S3 type	M13	25896	0.938	3.30
	M14	48561	0.95412	1.64
	M15	85467	0.95998	1.00
	M16	112847	0.97	-

At inlet 1: Constant inlet velocity v_0 and concentration of 0 are applied.

At inlet 2: Constant inlet velocity v_0 and concentration of 1 are applied.

At the wall: No slip and no penetration conditions are applied.

At outlet: Gauge pressure is considered as zero, and concentration outflow is considered. The mixing index for a given channel configuration is governed by mass Peclet number (Pe = ScRe).

4 Numerical methodology and model validation

The governing equations of conservations of mass, momentum and species transport are solved by a finite volume method-based solver. The second-order upwind scheme is used to discretize both the advection and diffusion terms. The SIMPLE algorithm is used for pressure-velocity coupling. The relative convergence criterion for the residuals is set to 10^{-5}. To design the 2D Y-shape square wave serpentine passive microchannel CATIA v5 software is used and ANSYS 14.0 FLUENT software is used to study the mixing behaviour of two fluids and pressure drop along the length of the channels.

Prior to numerical simulations, an extensive grid independence test has been carried out to minimize the computational time and resources without sacrificing the accuracy of the results. For each of the micromixer geometry, four different grid systems have been considered. The average density difference at a particular location (location 4) from the junction at the inlet velocity of 0.003 m/s for different grids is presented in Table 1. The simulations are performed with M3, M7, M11 and M15 grids for S0, S1, S2 and S3 type micromixers, respectively. For each geometry under consideration, an error analysis on the prediction of the results has been conducted by selecting the finest grid as a reference for that geometry. It is to be noted that the percentage difference of the results is less than 1% with respect to the reference grid system for the specific geometry.

Before presenting the findings of the current investigation, the accuracy of the present numerical solver used for the simulations ascertained. For validation purpose, first the geometry of the channel similar to the work of Miranda et al. (Miranda et al. 2010) is considered. Figure 3 presents the comparison of the mixing efficiency as obtained numerically from the current numerical simulations with that available in the literature (Miranda et al. 2010) for Re = 0.1, Pe = 1450, St = 3.33×10^{-2}. The excellent agreement in the results confirms the accuracy of the solver.
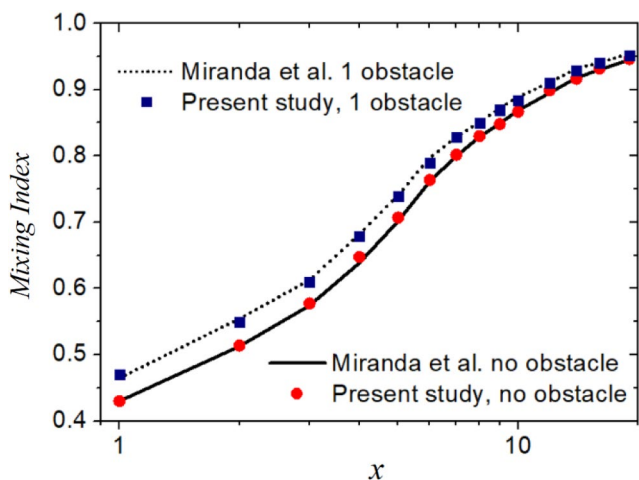
Fig. 3 Validation of simulation results against simulation results (Miranda et al. 2010)

5 Micromixer fabrication and experimental setup

CNC WEDM (Make: RATNAPARKHI (I) PVT. LTD., Nashik, India, Model: Ezeeecut NXG) has been used to fabricate different solid micromixer replica tools from the copper plate. These tools are then used as the pattern for making PDMS (SYLGARD (R) 184 SILICONE ELASTO-MER) micromixers by soft lithography technique. The inlet fluids have been injected through the fabricated micromixer by a twine syringe pump (Make: YASHTECH, Model: Mediflow-1000) with different flow rates. The mixing phenomena have been observed by an online camera system (DINO-LITE DIGITAL MICROSCOPE) with a computer. To measure the pressure, pressure sensor devices with a data logger (Make: Ideal Integrated Technology, India) have been connected at the inlet and outlet of the micromixer. The complete experimental setup which includes (a) syringe pump, (b) online monitoring system, (c) pressure sensor and data logger is shown in Fig. 4. Initially, fluid with three different flow rates is made to flow through simple serpentine square wave micromixer. Then the results are compared with that of mixers with obstructions.

6 Results and discussion

The computational analyses have been carried out for serpentine square wave micromixer without obstruction as well as with obstruction of three different shapes at three different inlet velocities (0.003 m/s 0.015 m/s and 0.030 m/s). At zero distance from the junction, the density difference between the two fluids is 211 kg/m^3. With increasing the channel length, the density difference decreases. When the density difference is equal to zero, the two liquids are assumed to mix perfectly.

6.1 Influence of channel geometry on mixing length

One can explain the effect of channel geometry on the mixing performance and pressure drop by analyzing the streamlines. Figure 5 represents the streamlines for all four types of micromixers at an inlet velocity of 0.003 m/s. It is seen from Fig. 5(a) that the streamlines are straight and parallel to each other for flow through micromixer without obstacles (S0 type). The streamlines become curved for flow through micromixers with obstacles, and the waviness of streamlines depends on the geometry of the obstacles (Falk and Commenge 2010; Commenge and Falk 2011). With the increase in the curvature of streamlines, fluids get mixed even though the flow is laminar. It is observed that the density difference between the two fluids gradually decreases in the downstream from the junction point, and finally, the density difference becomes zero. This is owing to the fact that the time of contact is more as the flow progresses. It
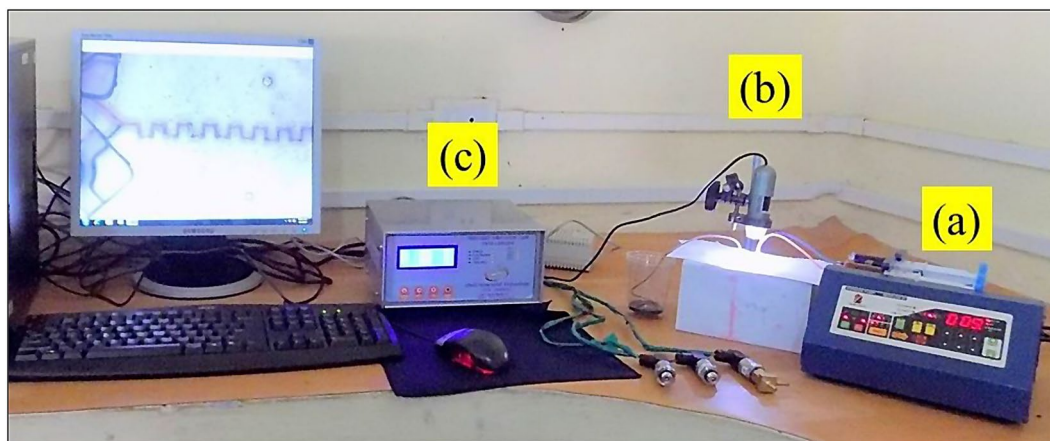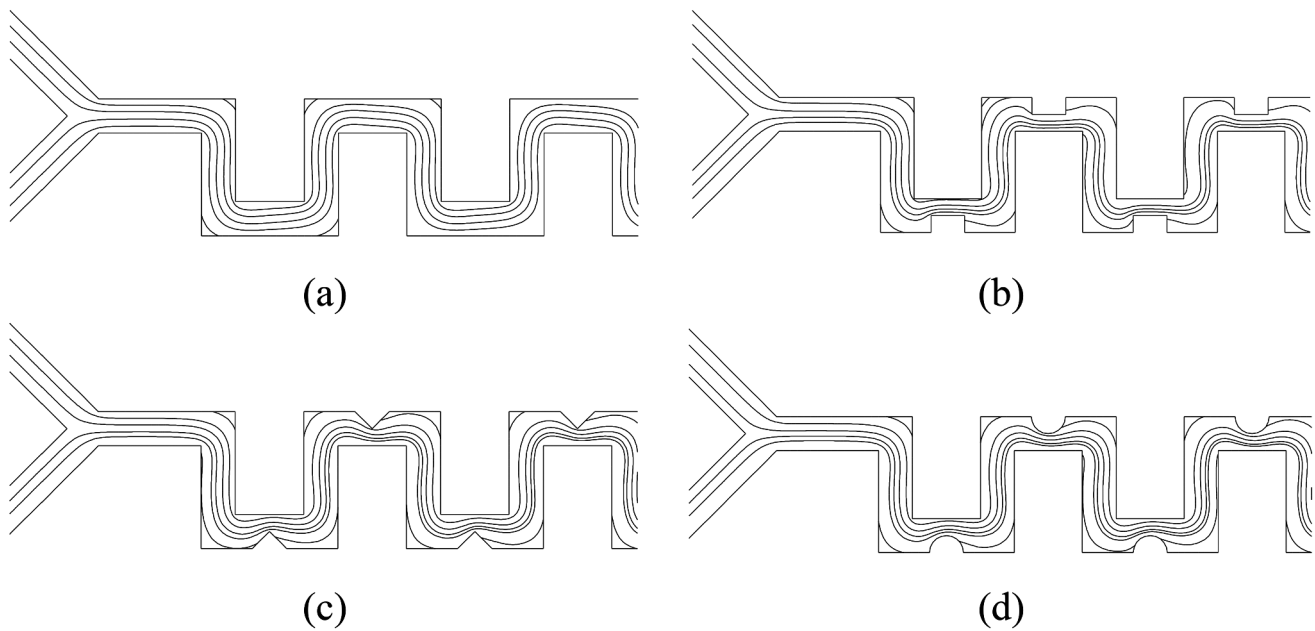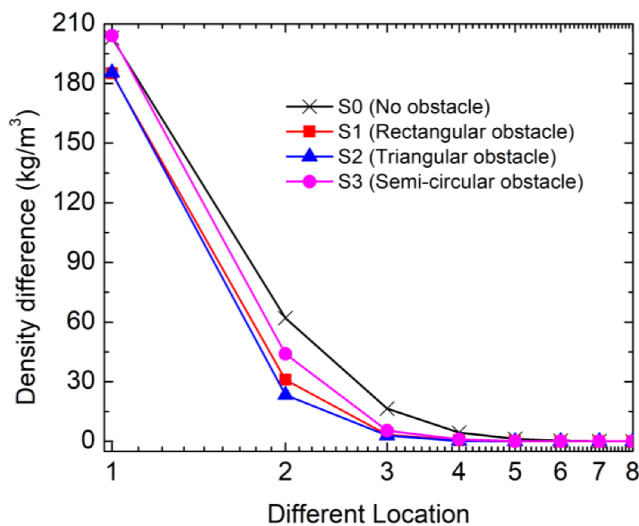

Fig. 4 Experimental setup for mixing

Fig. 5 Streamlines of serpentine square wave micromixers (**a**) without obstacle, with (**b**) rectangular, (**c**) triangular and (**d**) semicircular at velocity 0.003 m/s

Fig. 6 Density differences in different type microchannels while inlet velocity 0.003 m/s

is observed that for micromixers with obstacles of different shapes, density difference becomes zero for a shorter distance measured from the junction. This can be explained as follows. The aspect ratio of the mixer decreases in case of micromixer with obstacles (Song et al. 2012; Mondal et al. 2019b), as a result, fluids get mixed well, and it leads to better diffusion. This implies that the presence of obstacles in the mixer imparts quick mixing as compared to that of micromixer without obstacle(Jiang et al. 2004; Clark et al. 2018; Gidde et al. 2022). Though literally, obstruction means the higher flow resistance, here the presence of obstructions

is advantageous as far as better mixing is concerned(Gidde et al. 2018a,b). Comparing the mixing length of micromixers with various shape of obstacles, it is seen that the micromixer with triangular shape obstruction gives quick mixing as compared to that of other two as can be seen from Fig. 6.

## 6.2 Influence of inlet velocity on mixing length

A comparative study of mixing performance has been carried out by varying the inlet velocity for a particular microchannel geometry. The analysis is performed for S0 type micromixer with different inlet velocities of 0.003 m/s, 0.015 m/s and 0.030 m/s. The respective considered Reynolds numbers are 1, 5 and 10. It is observed that there is a significant difference in density at a particular location in S0 type micromixer while velocity of the fluid at the inlet is varied. Figure 7 shows the density difference for S0 type micromixer at different locations for different inlet velocities. It is seen that with the increase in inlet fluid velocity, mixing length decreases because of the fact that the strength of the recirculation gets enhanced with the inlet velocity.

6.3 Influence of channel geometry on pressure drop

The pressure drop is another important parameter that needs to be analyzed for efficient design of micromixers. The micromixer should operate in such a way that not only the mixing length is shorter but also have a relatively lower pressure drop. Intuitively, pressure drop depends on the flow velocity, and it increases with the increase in the velocity.
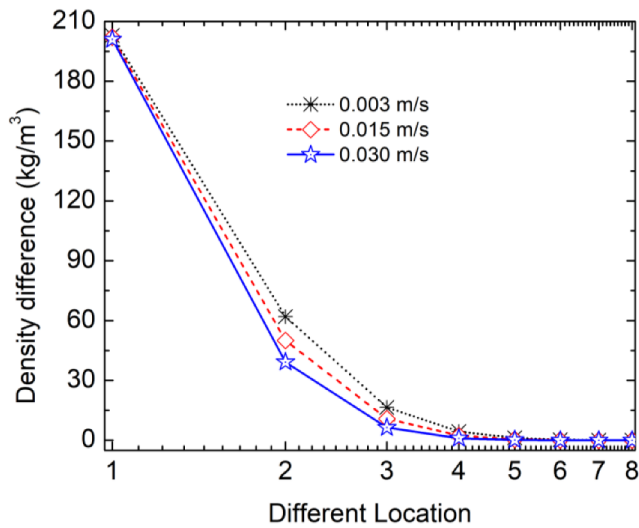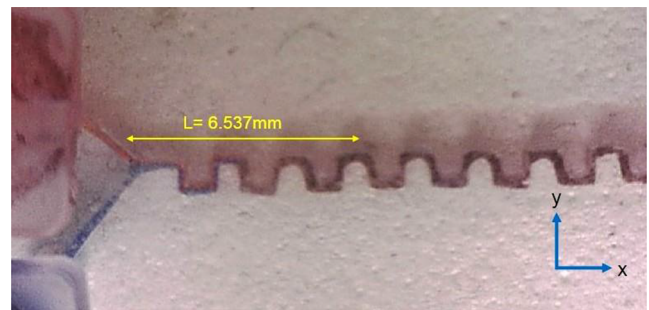
Fig. 7 Density differences in S0 type microchannels (inlet velocity (**a**) 0.003 m/s (**b**) 0.015 m/s (**c**) 0.03 m/s)
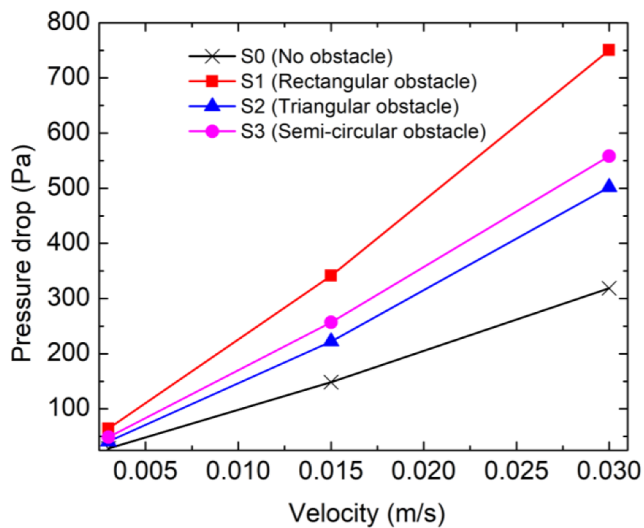
Fig. 8 Variation of pressure drop (Pa) obtained from computational study for different micromixers at different inlet velocities

The pressure drops in all four designed micromixers, i.e., S0, S1, S2, and S3 types have been calculated by varying the inlet velocity and is presented in Fig. 8. It is observed from Fig. 8 that the pressure drop in the micromixers with obstacles of different shape is higher as compared to that of micromixer without obstacle (S0 type). This is due to the fact that flow resistance due to the geometry of the flow passage increases due to the presence of the obstructions. It is seen that S1 type micromixer experiences the maximum pressure drop as compared to S2 and S3 type micromixers and the least pressure drop occurs in S2 type. Thus, S2 type of micromixer is preferable as far as minimum pressure drop criteria are concerned.
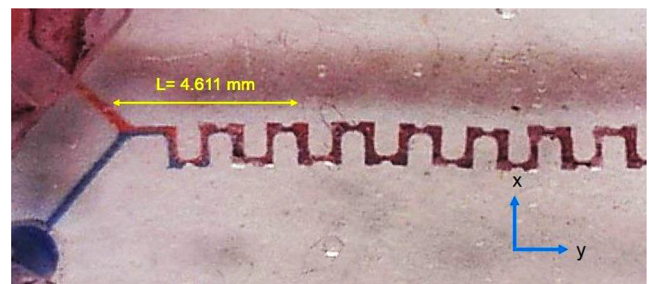

Fig. 9 Images of (**a**) S0, (**b**) S1, (**c**) S2 and (**d**) S3 type micromixer during experimentation

7 Experimental validation

In the experimental analysis, a little amount of red and blue inks/colours has been added to the fluids for better visualization of the characteristics. It is observed that at the junction point and at some distance from the junction, there is a clear separation between the two fluids. Here the mixing

Table 2 Density difference at different location from the junction while inlet velocity 0.003 m/s

Micromixer design	Location 1	Location 2	Location 3	Location 4	Location 5	Location 6	Location 7	Location 8
S0 type	203	62	16.5	4.4	1.24	0.305	0.078	0.0256
S1 type	185	31	3.34	0.519	0.074	0.0105	0	0
S2 type	185.5	23.3	2.9	0.213	0.019	0.008	0	0
S3 type	204	44	5.3	0.97	0.051	0.012	0	0

Density difference (kg/m^3) at different location from the junction

Table 3 Density difference at different location from the junction while inlet velocity 0.030 m/s

Micromixer design	Location 1	Location 2	Location 3	Location 4	Location 5	Location 6	Location 7	Location 8
S0 type	201	39.2	6.41	1.04	0.169	0.0275	0.004	0.001
S1 type	186	21.1	1.58	0.138	0.013	0	0	0
S2 type	186	16.6	1.3	0.063	0.005	0	0	0
S3 type	201	27.5	2.17	0.16	0.011	0	0	0

Density difference (kg/m^3) at different location from the junction

Table 4 Density differences at different location from the junction while inlet velocity 0.015 m/s

Micromixer design	Location 1	Location 2	Location 3	Location 4	Location 5	Location 6	Location 7	Location 8
S0 type	202	50	10.8	2.34	0.5	0.109	0.024	0.005
S1 type	185.5	25.8	2.6	0.326	0.044	0.005	0	0
S2 type	186	20.3	2.16	0.133	0.012	0	0	0
S3 type	202	36.5	3.7	0.36	0.028	0.004	0	0

Density difference (kg/m^3) at different location from the junction

Table 5 Mixing length for different type of micromixers obtained from experiments

Type of Micromixer	S0 type	S1 type	S2 type	S3 type
Mixing length, L (mm)	6.537	4.605	4.491	4.611
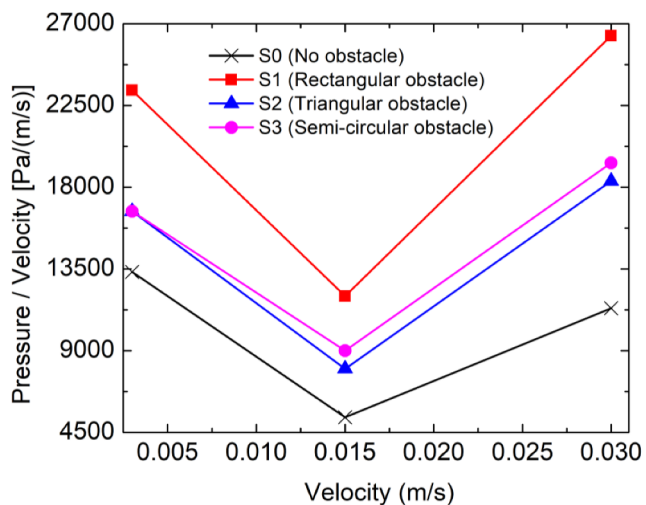
Fig. 10 Variation of pressure drop (Pa)/ velocity (m/s) obtained from experiments for different micromixers at different inlet velocities

point is measured offline from the images as captured by an online camera. The observations have been done from the inlet side. A measurement line is drawn from the junction point to that location which indicates the mixing length. The mixing length at a flow rate of 0.003 m/s for different types of micromixers is shown in Fig. 9. A comparison of

the mixing length obtained from experimental analyses is shown in Table 2.

From the experimental analysis, it is also seen that the pressure drop in serpentine square wave micromixer with obstacles is higher as compared to that of micromixer without obstacle. Comparing pressure drop among the micromixers having serpentine square wave with different obstacles such as S1, S2, S3 type, it is observed that in S2 type micromixer experiences less pressure drop (Fig. 10). With respect to pressure drop in different types of micromixer with an obstacle, S2 type of micromixer is the most preferable due to less pressure drop in it.

The obtained results from the experimental analysis are not exactly same when compared to those of computational analysis due to some system limitations. There are some differences due to various experimental conditions such as micromixer material, dimensions, edge smoothness, working temperature, low magnifying imaging system, accuracy of the syringe pump, higher least count of the available data logger and monitoring device, etc. The deviation values of mixing length are varied from 0.5 to 7.2%, and the mean deviation is 2.61%. The comparison between the experimental and computational values of pressure drop (Pa) for different design micromixer at different inlet velocity is shown in Fig. 11. For pressure drop calculation by comparing all the cases, it is observed that the mean deviation is 9.4%. It is also observed that the higher deviations are found in case lower values of pressure drop and the higher least count readability is the main reason for this.
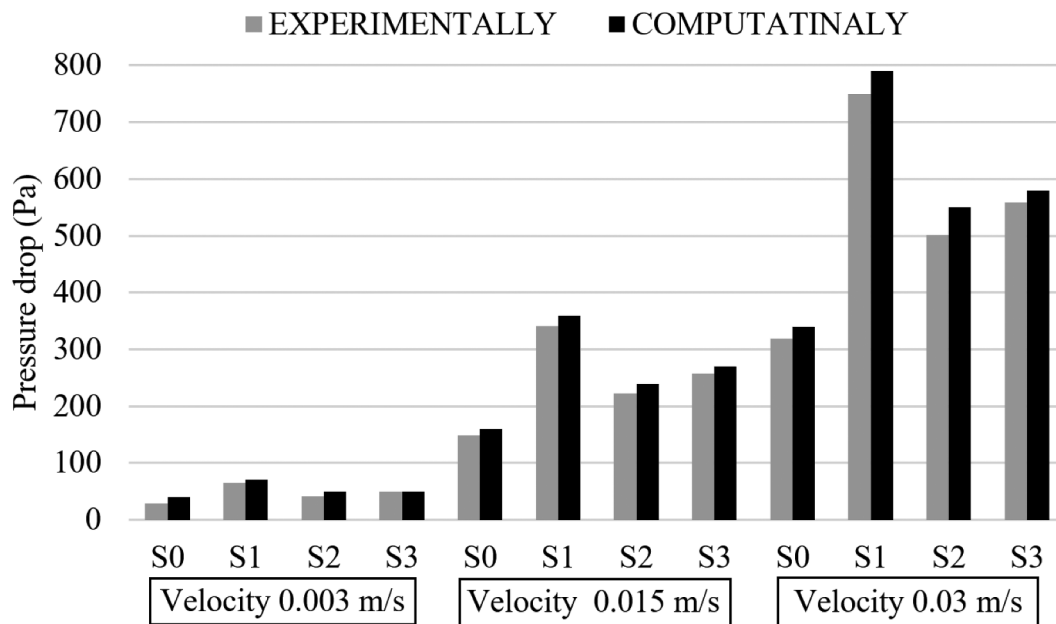
Fig. 11 Comparison of values of the pressure drop (Pa) for different micromixers at different inlet velocities obtained from the experimental and computational investigations

8 Conclusions

In this work, numerical and experimental investigations have been performed in serpentine square wave micromixer with and without obstructions along the width to analyze the mixing length and pressure drop. Three different shapes of the obstacles, namely, rectangular, triangular and semicircular, are considered. The main findings from the present work are summarized as follows:

- Placing obstacles in the micromixer creates disordered advection effect, which is a novel method to shorten the mixing length in passive micromixers.
- Micromixer with any shape of obstruction shows rapid mixing as compared to that of without obstruction.
- The mixing length decreases by 29.57%, 31.29% and 29.46% in micromixer with rectangular, triangular, and semicircular shape obstacle respectively as compared to micromixer without obstacle.
- The pressure drop increases in case of obstacles in the micromixer compared to the case without obstacle.
- The micromixer with triangular shape obstruction gives the minimum mixing length, while the corresponding pressure drop is also the lowest among all the micromixers with obstacles.

References

Ang KM, Yeo LY, Hung YM, Tan MK (2016) Amplitude modulation schemes for enhancing acoustically-driven microcentrifugation and micromixing. Biomicrofluidics 10:054106. https://doi.org/10.1063/1.4963103

Ballard M, Owen D, Mills ZG et al (2016) Orbiting magnetic microbeads enable rapid microfluidic mixing. Microfluid Nanofluidics 20:1–13. https://doi.org/10.1007/s10404-016-1750-1

Bayareh M, Ashani MN, Usefian A (2020) Active and passive micromixers: a comprehensive review. Chem Eng Process - Process Intensif 147:107771

Borgohain P, Arumughan J, Dalal A, Natarajan G (2018a) Design and performance of a three-dimensional micromixer with curved ribs. Chem Eng Res Des 136:761–775. https://doi.org/10.1016/j.cherd.2018.06.027

Borgohain P, Choudhary D, Dalal A, Natarajan G (2018b) Numerical investigation of mixing enhancement for multi-species flows in wavy channels. Chem Eng Process - Process Intensif 127:191–205. https://doi.org/10.1016/j.cep.2018.03.026

Calado B, dos Santos A, Semiao V (2016) Characterization of the mixing regimes of newtonian fluid flows in asymmetrical T-shaped micromixers. Exp Therm Fluid Sci 72:218–227. https://doi.org/10.1016/j.expthermflusci.2015.11.010

Chen X, Li T, Zeng H et al (2016) Numerical and experimental investigation on micromixers with serpentine microchannels. Int J Heat Mass Transf 98:131–140. https://doi.org/10.1016/j.ijheatmasstransfer.2016.03.041

Clark J, Kaufman M, Fodor PS (2018) Mixing Enhancement in Serpentine Micromixers with a Non-Rectangular Cross-Section. Micromachines 2018, Vol 9, Page 107 9:107. https://doi.org/10.3390/MI9030107

Commenge JM, Falk L (2011) Villermaux–Dushman protocol for experimental characterization of micromixers. Chem Eng Process Process Intensif 50:979–990. https://doi.org/10.1016/J.CEP.2011.06.006

Connolly P (1995) Clinical diagnostics opportunities for biosensors and bioelectronics. Biosens Bioelectron 10:1–6. https://doi.org/10.1016/0956-5663(95)96789-2

Das SS, Tilekar SD, Wangikar SS, Patowari PK (2017) Numerical and experimental study of passive fluids mixing in micro-channels of different configurations. Microsyst Technol 23:5977–5988. https://doi.org/10.1007/s00542-017-3482-x

Deshmukh AA, Liepmann D, Pisano AP et al (2000) Continuous micromixer with pulsatile micropumps. pp 73–76

Falk L, Commenge JM (2010) Performance comparison of micromixers. Chem Eng Sci 65:405–411. https://doi.org/10.1016/J.CES.2009.05.045

Gambhire S, Patel N, Gambhire G, Kale S (2016) A review on different micromixers and its Micromixing within Microchannel. Int J Curr Eng Technol 409–413. https://doi.org/10.13140/RG.2.1.4235.4324

Gidde RR, Pawar PM, Ronge BP et al (2018a) Evaluation of the mixing performance in a planar passive micromixer with circular and square mixing chambers. Microsyst Technol 24:2599–2610. https://doi.org/10.1007/s00542-017-3686-0

Gidde RR, Shinde AB, Pawar PM, Ronge BP (2018b) Design optimization of a rectangular wave micromixer (RWM) using Taguchi based grey relational analysis (GRA). Microsyst Technol 24:3651–3666. https://doi.org/10.1007/s00542-018-3815-4

Gidde RR, Wangikar SS, Pawar PM, Ronge BP (2022) A comparative study: conventional and modified serpentine micromixers. Chem Prod Process Model 18:521–539. https://doi.org/10.1515/CPPM-2022-0022/MACHINEREADABLECITATION/RIS

Huang C, Tsou C (2014) The implementation of a thermal bubble actuated microfluidic chip with microvalve, micropump and micromixer. Sens Actuators Phys 210:147–156. https://doi.org/10.1016/j.sna.2014.02.015

Jakeway SC, De Mello AJ, Russell EL (2000) Miniaturized total analysis systems for biological analysis. Fresenius J Anal Chem 366:525–539

Jiang F, Drese KS, Hardt S et al (2004) Helical flows and chaotic mixing in curved micro channels. AIChE J 50:2297–2305. https://doi.org/10.1002/AIC.10188

Khosravi Parsa M, Hormozi F, Jafari D (2014) Mixing enhancement in a passive micromixer with convergent-divergent sinusoidal microchannels and different ratio of amplitude to wave length. Comput Fluids 105:82–90. https://doi.org/10.1016/j.compfluid.2014.09.024

Kunti G, Bhattacharya A, Chakraborty S (2017) Rapid mixing with high-throughput in a semi-active semi-passive micromixer. Electrophoresis 38:1310–1317. https://doi.org/10.1002/elps.201600393

Kunti G, Bhattacharya A, Chakraborty S (2018) Electrothermally actuated moving contact line dynamics over chemically patterned surfaces with resistive heaters. Phys Fluids 30:062004. https://doi.org/10.1063/1.5028172

Lee CY, Fu LM (2018) Recent advances and applications of micromixers. Sens Actuators B Chem 259:677–702

Mehta SK, Pati S (2022) Enhanced electroosmotic mixing in a wavy micromixer using surface charge heterogeneity. Ind Eng Chem Res 61(7):2904–2914. https://doi.org/10.1021/acs.iecr.1c04318

Mehta SK, Mondal B, Pati S, Patowari PK (2022) Enhanced electroosmotic mixing of non-newtonian fluids in a heterogeneous surface charged micromixer with obstacles. Colloids Surf Physicochem Eng Asp 648:129215. https://doi.org/10.1016/J.COLSURFA.2022.129215

Miranda JM, Oliveira H, Teixeira JA et al (2010) Numerical study of micromixing combining alternate flow and obstacles. Int Commun Heat Mass Transf 37:581–586. https://doi.org/10.1016/j.icheatmasstransfer.2010.01.012

Mondal B, Pati S, Patowari PK (2018) Effect of Confluence Angle between Inlets on the Mixing Characteristics in Microchannel. In: Proceedings of the 7th International and 45th National Conference on Fluid Mechanics and Fluid Power. IIT Bombay, India, 12–14 Dec, p 64

Mondal B, Mehta SK, Patowari PK, Pati S (2019a) Numerical study of mixing in wavy micromixers: comparison between raccoon and serpentine mixer. Chem Eng Process - Process Intensif 136:44–61. https://doi.org/10.1016/j.cep.2018.12.011

Mondal B, Pati S, Patowari P (2019b) Analysis of mixing performances in microchannel with obstacles of different aspect ratios. Proc Inst Mech Eng Part E J Process Mech Eng 233:1045–1051. https://doi.org/10.1177/0954408919826748

Mondal B, Pati S, Patowari PK (2020a) Numerical Analysis of Mixing Performance in Microchannel with different ratio of outlet to Inlet Width. Techno-Societal 2018. Springer International Publishing, pp 257–266

Mondal B, Pati S, Patowari PK (2020b) Fabrication of wavy micromixer using soft lithography technique. Mater Today Proc 26:1271–1278. https://doi.org/10.1016/j.matpr.2020.02.254

Mondal B, Pati S, Patowari PK (2020c) Assessment of mixing in microchannel with obstacles. In: International Conference on Energy and Sustainable Development 2020. JU, Kolkata, India, 14–15 Feb, pp 241–244 ISBN 978-93-83660-56–8

Mondal B, Pati S, Patowari PK (2020d) Influence of Confluence Angle between inlets on the Mixing performance of micro-mixer with obstacles. Techno-Societal 2018. Springer International Publishing, pp 275–283

Mondal B, Mehta SK, Pati S, Patowari PK (2021) Numerical analysis of electroosmotic mixing in a heterogeneous charged micromixer with obstacles. Chem Eng Process Process Intensif 168:108585. https://doi.org/10.1016/j.cep.2021.108585

Nguyen NT, Wu Z (2005) Micromixers—a review. J Micromechanics Microengineering 15:1–16

Pérez K, Picard B, Vuluga D et al (2020) Bromine-Lithium Exchange on a gem-Dibromoalkene, part 2: comparative performance of Flow Micromixers. Org Process Res Dev 24:787–791. https://doi.org/10.1021/ACS.OPRD.0C00203/SUPPL_FILE/OP0C00203_SI_001.PDF

Pinot J, Commenge JM, Portha JF, Falk L (2014) New protocol of the villermaux–Dushman reaction system to characterize micromixing effect in viscous media. Chem Eng Sci 118:94–101. https://doi.org/10.1016/J.CES.2014.07.010

Rashidi S, Bafekr H, Valipour MS, Esfahani JA (2018) A review on the application, simulation, and experiment of the electrokinetic mixers. Chem Eng Process Process Intensif 126:108–122

Sarma P, Patowari PK (2017) Study on design modification of Serpentine Micromixers for Better Throughput for Microfluidic Circuitry. Micro Nanosyst 8:119–125. https://doi.org/10.2174/1876402909666170217151907

Song H, Wang Y, Pant K (2012) Cross-stream diffusion under pressure-driven flow in microchannels with arbitrary aspect ratios: a phase diagram study using a three-dimensional analytical model. Microfluid Nanofluidics 12:265–277. https://doi.org/10.1007/s10404-011-0870-x

Tsai TH, Liou DS, Kuo LS, Chen PH (2009) Rapid mixing between ferro-nanofluid and water in a semi-active Y-type micromixer. Sens Actuators Phys 153:267–273. https://doi.org/10.1016/j.sna.2009.05.004

Vasista KN, Mehta SK, Pati S (2022) Electroosmotic mixing in a microchannel with heterogeneous slip dependent zeta potential. Chem Eng Process Process Intensif 176:108940. https://doi.org/10.1016/j.cep.2022.108940

Wangikar SS, Patowari PK, Misra RD (2018) Numerical and experimental investigations on the performance of a serpentine

microchannel with semicircular obstacles. Microsyst Technol 24:3307–3320. https://doi.org/10.1007/s00542-018-3799-0

Yang Z, Matsumoto S, Goto H et al (2001) Ultrasonic micromixer for microfluidic systems. Sens Actuators Phys 93:266–272. https://doi.org/10.1016/S0924-4247(01)00654-9